INFRARED PHOTOCATHODE

H. Sonnenberg

GTE Sylvania, Incorporated

Prepared for:

Advanced Research Projects Agency

31 December 1971

INFRARED PHOTOCATHODE

SEMI-ANNUAL TECHNICAL REPORT

ARPA Order Number:	1806
Program Code Number:	00014
Contractor:	GTE Sylvania Inc.
Effective Date:	1 November 1969
Expiration Date:	30 April 1972
Contract Amount:	$178,686
Contract Number:	N00014-70-C-0079
Principal Investigator:	Dr. H. Sonnenberg
Telephone:	(415) 966-3472
Scientific Officer:	Dr. Robert E. Behringer

Sponsored by
Advanced Research Projects Agency
ARPA Order No. 1806

Prepared by

H. Sonnenberg
Electro-Optics Research and
Development Department

Approved by

L. M. Osterink, Manager
Electro-Optics Research and
Development Department

DOCUMENT CONTROL DATA - R & D

(Security classification of title, body of abstract and indexing annotation must be entered when the overall report is classified)

1. ORIGINATING ACTIVITY (Corporate author)

GTE Sylvania Inc.

2a. REPORT SECURITY CLASSIFICATION

UNCLASSIFIED

2b. GROUP

3. REPORT TITLE

Infrared Photocathode

4. DESCRIPTIVE NOTES (Type of report and inclusive dates)

Semi-Annual Report May 1 - Nov. 30, 1971

5. AUTHOR(S) (First name, middle initial, last name)

H. Sonnenberg

6. REPORT DATE	7a. TOTAL NO. OF PAGES	7b. NO. OF REFS
Dec. 31, 1971	~~21~~ 23	14

8a. CONTRACT OR GRANT NO.	9a. ORIGINATOR'S REPORT NUMBER(S)
N00014-70-C-0079	None
b. PROJECT NO.	
c.	9b. OTHER REPORT NO(S) (Any other numbers that may be assigned this report)
d.	None

10. DISTRIBUTION STATEMENT

Unlimited

11. SUPPLEMENTARY NOTES	12. SPONSORING MILITARY ACTIVITY
None	Advanced Research Projects Agency

13. ABSTRACT

Efficient photoemission from $InAs_{1-x}P_x$ (Cs-O) with a bandgap-limited threshold at 1.4 microns was observed. Indirect measurements of the composition and thickness of the Cs-O low-work-function surface show that the surface consists of about one monolayer of Cs, followed by approximately one monolayer of cesium oxide. These data make an interpretation of the low-work-function properties of Cs-O in terms of the heterojunction model (based on the bulk properties of Cs_2O) questionable.

The escape probability as a function of wavelength for NEA photoemitters is calculated with the aid of the heterojunction model. The theoretical escape probabilities are in good qualitative and quantitative agreement with the experimental values. It is shown that recently reported photoemission out to 1.3 microns is not in disagreement with the heterojunction model.

Vapor phase epitaxy of GaAs on Ge, Spinel and GaAs substrates is briefly discussed.

DD FORM 1 NOV 1473 REPLACES DD FORM 1473, 1 JAN 64, WHICH IS OBSOLETE FOR ARMY USE.

Security Classification

14. KEY WORDS	LINK A		LINK B		LINK C	
	ROLE	WT	ROLE	WT	ROLE	WT
Photoemission						
Photocathodes						
Cesium Oxide						
Heterojunctions						
Vapor Epitaxy						
Infrared Detector						

Security Classification

TECHNICAL REPORT SUMMARY

The technical objective of this program is the development of an efficient photocathode for the 1.5 micron region of the infrared spectrum. No such photocathode exists today. The concept of the heterojunction photocathode proposed by us earlier[1], represented a new approach to the development of an infrared cathode.

This approach, exploited on this contract, led to the discovery of the most efficient (at that time) 1.06 micron photocathode[2]. Further improvements in this cathode have been made, and even today it remains the most efficient 1.06 micron photocathode yet developed. Continued development of infrared cathodes on this project has led to photocathodes having, for the first time, usable response out to 1.3 microns, see Section 1.0.

In Section 1.0 of this report we summarize our results on the long-wavelength photoemission from "heterojunction-type" cathodes. Theoretical implications of our results are also given. In Section 2.0, the escape probability, which is the major determining factor in the efficiency of these cathodes is calculated and compared to the experimental data out to 1.4 microns. It is shown that the peak quantum efficiency to be expected at 1.5 microns is on the order of 0.01%. Although this may be useful in certain applications, it is not considered adequate to warrant further development. Thus, we have abandoned the simple "heterojunction" cathode approach in favor of an approach which provides for optical absorption in a small bandgap material which is in contact with a large bandgap material known to have a high electron escape probability.

---

(1) H. Sonnenberg, Appl. Phys. Letters 14 289 (1969).

(2) Quarterly Management Report #1 (Feb. 10, 1970); H. Sonnenberg, Appl. Phys. Letters 16, 245 (1970).

The first step in this approach is the epitaxial growth of materials. This work is discussed in Section 3.0. Infrared photocathodes with 1% or better efficiency at 1.5 microns appear feasible by this approach.

1.0 LONG-WAVELENGTH PHOTOEMISSION FROM $InAs_{1-x}P_x$

In early 1970 we reported[1] the discovery of the $InAs_{0.15}P_{0.85}$ photocathode, which at the time was the most efficient 1.06 micron photoemitter yet developed. This was the first major step in the development of infrared cathodes on this program. Since then, James et al[2] have achieved even higher quantum yields at 1.06 microns in better quality $InAs_{1-x}P_x$. Comparable results were reported by Fisher et al,[3] in $Ga_{1-x}In_xAs$. In each case, the photocathode surface was treated with Cs and O_2 to lower the work function of the cathode material to establish a negative-electron-affinity condition. Although the experimental results reported by different investigators have been roughly comparable, the function of the Cs and O_2 in lowering the work function of the photocathode material has recently been the subject of considerable controversy. On the one hand is the interpretation in terms of the heterojunction model[4,5] which ascribes bulk properties to a Cs_2O layer assumed to be present in the low-work function surface. On the other hand is the interpretation in terms of a surface dipole layer of Cs and O_2 (6,3). In this section we present our results on the long-wavelength response of $InAs_{1-x}P_x$ photocathodes and report on indirect measurements of the thickness and composition of the Cs-O low-work-function surface.

The infrared photoresponse of three different $InAs_{1-x}P_x$ photocathodes developed on this project is shown in Figure 1. Curve 1 is repeated from reference 1 and curves 2 and 3 represent our more recent results on $InAs_{0.25}P_{0.75}$ and $InAs_{0.4}P_{0.6}$ respectively. Curve 3 is of most interest since it shows relatively-efficient, bandgap-limited photoemission out to 1.4 microns. At 1.3 microns, the quantum yield of this cathode is 0.016%.

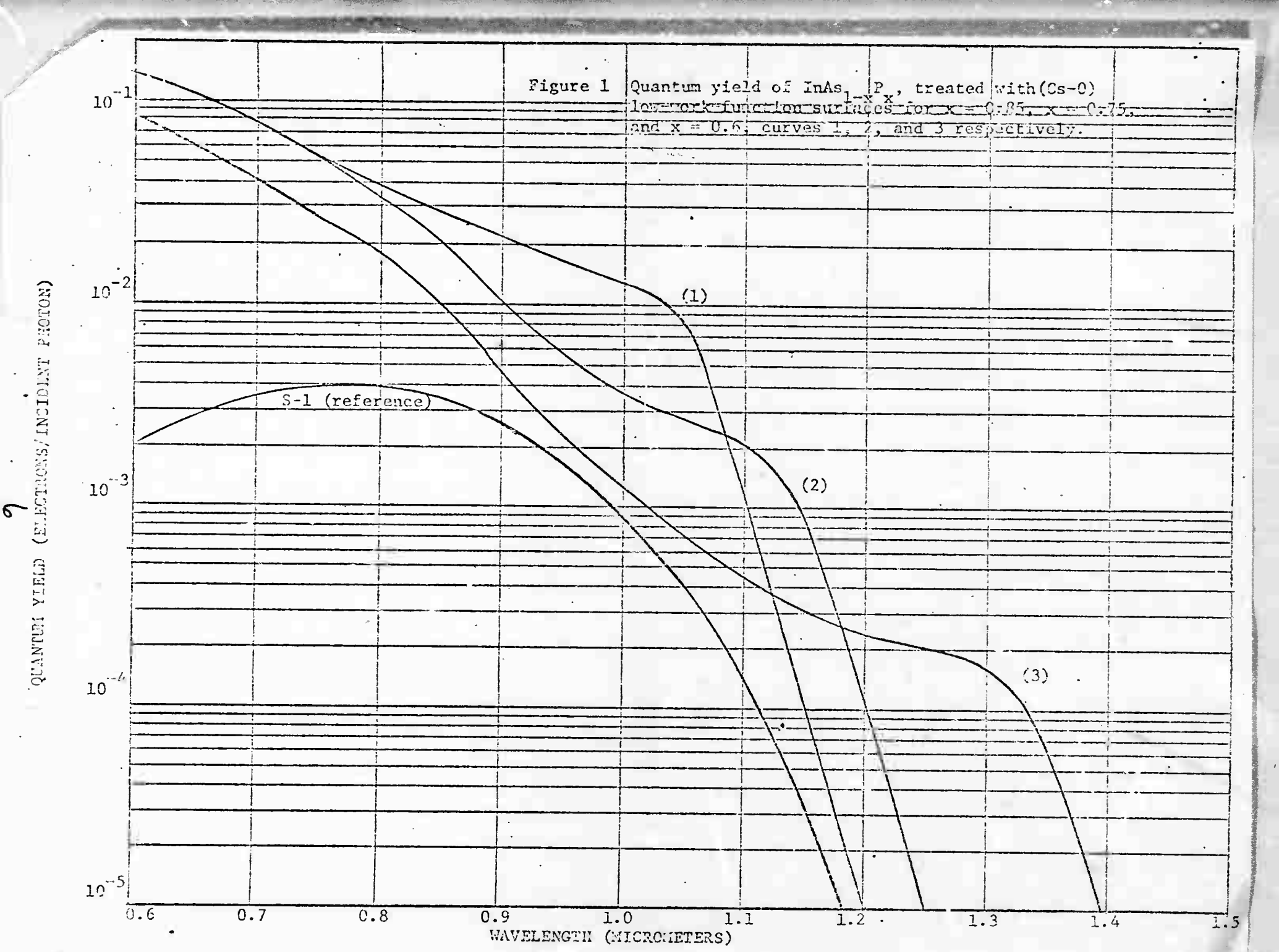
Figure 1 Quantum yield of $InAs_{1-x}P_x$, treated with (Cs-O) low-work-function surfaces for x = 0.85, x = 0.75, and x = 0.6; curves 1, 2, and 3 respectively.
QUANTUM YIELD (ELECTRONS/INCIDENT PHOTON) η
10^{-1}
10^{-2}
10^{-3}
10^{-4}
10^{-5}
S-1 (reference)
(1)
(2)
(3)
0.6
0.7
0.8
0.9
1.0
1.1
1.2
1.3
1.4
1.5
WAVELENGTH (MICROMETERS)

In the past, we have attempted to explain our results in terms of the heterojunction model, the validity of which has now been questioned[6,3]. The major objection to the heterojunction model was raised by direct-chemical analysis[6] of the Cs content of GaAs (Cs) and GaAs (Cs-O) photocathodes. It was shown that if Cs_2O is formed at all, peak sensitivity is reached with the equivalent of one monolayer of Cs and one monolayer of Cs_2O. Clearly the Cs-O low-work-function-surface properties are difficult to explain with a model based on the bulk properties of Cs_2O, when only one monolayer of Cs_2O is present.

We have indirectly measured the thickness of the Cs-O low-work-function surface on $InAs_{1-x}P_x$ by a different technique and find, in agreement with Sommer et al[6], that the Cs-O layers may be sufficiently thin to make the heterojunction interpretation questionable. The thickness was estimated as follows: The Cs generation rate was first stabilized. Next, the $InAs_{1-x}P_x$ crystal was cleaved and the time taken to optimize the surface with Cs only recorded. Maintaining this set Cs rate, O_2 was then introduced simultaneously at an exposure level such that the rate of increase in photoemission from the cathode was maximized. The total O_2 exposure was measured with an Ultek Partial Pressure Analyzer by integrating over the exposure period. To determine the total Cs and O_2 exposure, we assume that the Cs and O_2 sticking coefficients do not change significantly with coverage.

Sensitization of electron-affinity photocathodes by the simultaneous exposure to Cs and O_2 described above, differs from the standard method which involves the alternate application of Cs and O_2. We have been using the simultaneous-exposure technique for a number of years now and find that in our work, this method gives better results, particularly with smaller bandgap materials. The

philosophy behind the technique is that for a given rate of Cs exposure, the O_2 exposure should be adjusted to give a maximum rate of increase in photoemission in order to minimize the thickness of the low-work-function surface. This in turn would maximize the escape probability, and thereby optimize the photoresponse.

It seems likely that at least part of the controversy over Cs-O low-work-function surfaces is due to differences in the processing technique. In our work the simultaneous technique was used exclusively.

Table I summarizes our findings for $InAs_{0.25}P_{0.75}$. The first two columns of data give the ratio of cesium to oxygen assuming that all cesium is converted to oxide[7]. The first column gives the ratio of cesium to oxygen for the case in which the photoresponse is optimized at 6328Å, and the second column gives the ratio for the case in which the photoresponse is optimized at 10,000Å. If a stochiometric Cs-O compound is formed[5], then this ratio should remain constant. The ratio does not remain constant. However, the ratio of cesium to oxygen given in the next two columns, where it is assumed that one monolayer[8] of Cs is not converted to oxide, remains relatively constant, suggesting that our Cs-O low-work-function surfaces consist of a cesium layer and an oxide layer, the Cs layer being slightly less than a monolayer thick[9]. If we assume that the oxide is Cs_2O, then the thickness of the low-work-function layer can be estimated from the Cs exposure and the relative bulk densities of the Cs_2O and of the Cs. The coverage, in terms of monolayers of Cs and Cs_2O are given in the last two columns.

The photoyield in the visible (6328Å) is optimized with a coverage of only about 1 monolayer of Cs and 0.8 monolayers of Cs_2O. This case should correspond most closely to the coverage required for GaAs and is in excellent agreement with the findings of Sommer et al[6] for GaAs. However, when the photoyield is optimized at 10,000Å the coverage increases to approximately 1 monolayer of Cs and 1.4 monolayers of Cs_2O. Apparently thicker cesium oxide coverage is necessary to optimize the photoresponse of smaller-bandgap materials. This is in contrast to the claim made in Ref. 3.

SAMPLE NUMBER	RATIO[1] Cs/O		RATIO[2] Cs/O		COVERAGE[2] (MONOLAYERS)	
	.6328 opt.	1.0 opt.	.6328 opt.	1.0 opt.	.6328 opt.	1.0 opt.
1	(0.77)Y	(0.67)Y	(0.47)Y	(0.51)Y	(1) Cs + (0.7) Cs_2O	(1) Cs + 1.4 Cs_2O
2	(0.78)Y	(0.82)Y	(0.51)Y	(0.63)Y	(1) Cs + (0.8) Cs_2O	(1) Cs + (1.4) Cs_2O
3	(0.74)Y	(0.66)Y	(0.49)Y	(0.52)Y	(1) Cs + (0.8) Cs_2O	(1) Cs + (1.6) Cs_2O
4	(0.69)Y	(0.67)Y	(0.48)Y	(0.51)Y	(1) Cs + (0.9) Cs_2O	(1) Cs + (1.4) Cs_2O

(1) ASSUMING ALL Cs IS CONVERTED TO OXIDE

(2) ASSUMING ONE MONOLAYER OF Cs IS NOT CONVERTED

Table I Ratio of cesium to oxygen and Cs-O low-work-function coverage for $InAs_{0.25}P_{0.75}$ optimized at 6328Å and at 10,000Å. The factor Y is a constant multiplier[7]

Figure 2 shows the effect of the thicker oxide layer on the photoresponse of sample number 1. The response in the visible spectrum decreases, whereas the threshold reponse increases. The decrease in the response is likely the result of increased electron scattering in the thicker oxide layer and the increase in the infrared yield is probably associated with a decrease in the work function of the Cs-O surface which more than compensates for the increased scattering in the thicker layer.

Subject to the assumptions implied in this paper, the following conclusions can be reached:

1) Relatively efficient photoemission with a bandgap-limited-threshold at 1.4 microns can be achieved in $InAs_{1-x}P_x$.
2) The low-work-function Cs-O surface probably consists of a Cs layer slightly less than a monolayer thick, followed by an oxide layer of monolayer dimensions.
3) For optimum infrared response, small bandgap materials require thicker oxide coatings than do larger bandgap materials.

The fact that relatively efficient photoemission was observed with a bandgap-limited threshold at 1.4 microns shows that earlier predictions[10] of the long-wavelength limit of Cs-O covered photocathodes have overemphasized the influence of the interfacial barrier (if it exists). Furthermore, since the thickness of the Cs-O low-work-function surface appears to be of monolayer proportions, the concept of the heterojunction cathode [4,5] based on the bulk properties of Cs_2O if used at all, must be used with caution. However, in contrast to a previous interpretation of bandgap-limited photoemission out to 1.3 microns[3], as shown in Section 2.0[11], bandgap-limited photoemission out to 1.4 microns can not be taken as evidence for the absence of an interfacial barrier, nor evidence for an interfacial-barrier height less than 0.89 eV.

Figure 1 Quantum yield of $InAs_{0.25}Sb_{0.85}$ optimized at 9500Å (broken curve) compared to the yield obtained on the same sample when the processing is continued until the yield at 10,000Å is optimized (solid curve).

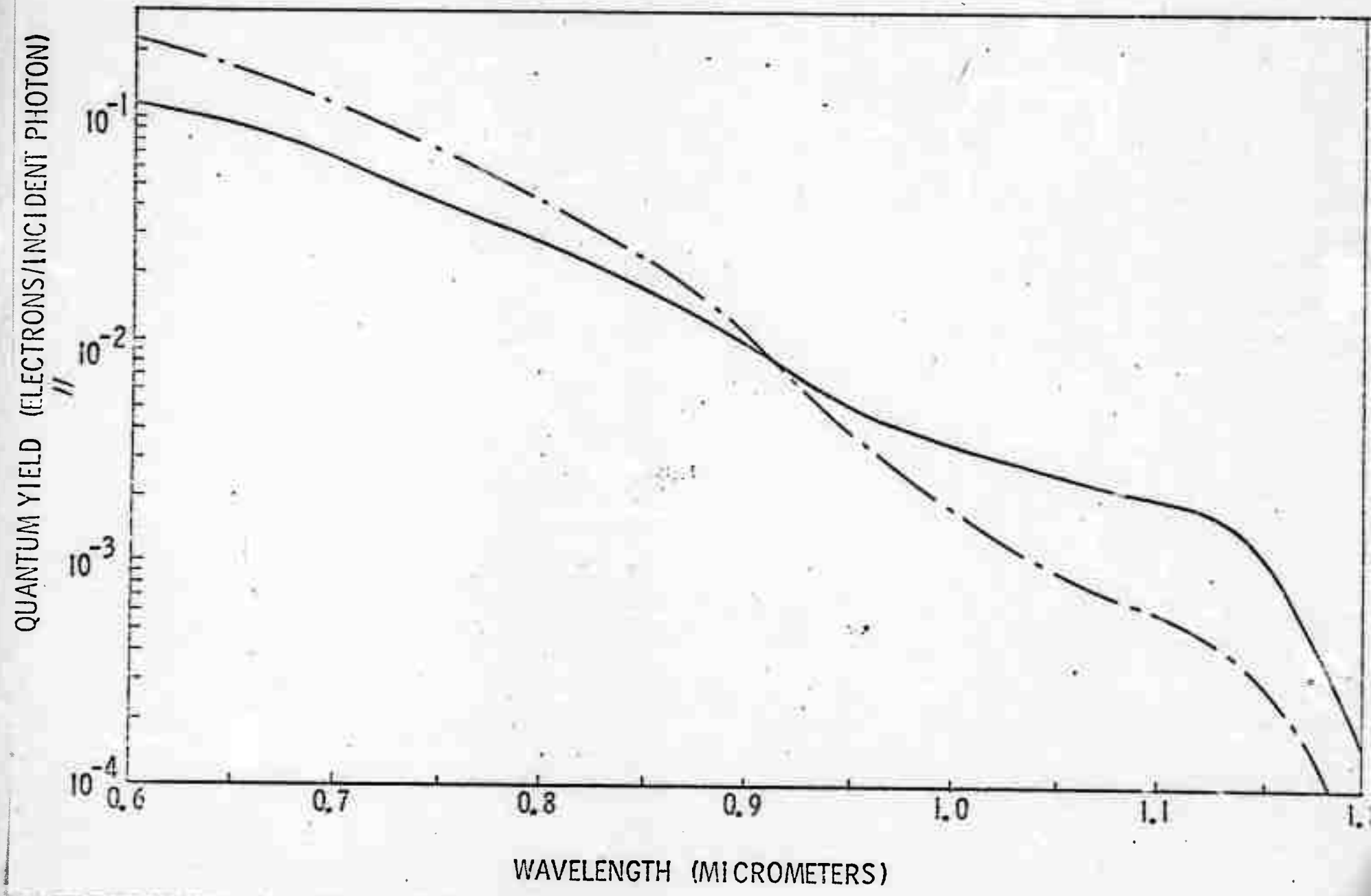

2.0 ESCAPE PROBABILITY OF NEGATIVE-ELECTRON-AFFINITY PHOTOEMITTERS

Fisher et al[3] recently reported bandgap-limited photoemission out to 1.3 microns. They, along with Williams and Tietjen[12], take this as evidence for either the absence of an interface barrier or for an internal barrier considerably smaller than 0.96 eV. They conclude further that this is evidence against the heterojunction interpretation of photoemission from NEA cathodes. In this section, we show that the results of Fisher et al[3] can be adequately interpreted within the framework of the heterojunction photocathode[4,5], containing a non-zero interface-barrier. Settlement of this question is important in establishing confidence limits in the theoretical predictions of the infrared-yield for cathodes utilizing Cs-O low-work-function surfaces.

The simple energy-band-vs-position diagram of the heterojunction model shown in Figure 3 forms the basis for our calculations. One of the important simplifying assumptions in our calculations is that the structure and all processes are one dimensional. The NEA structure consists of three regions: the bulk or absorbing material, the low-work-function surface-material, and vacuum. Both the bulk and surface regions are divided into flat-band and non-flat-band portions. The interface barrier (at $x = a$) and the surface barrier (at $x = a + b$) are the two features which most strongly influence photoemission.

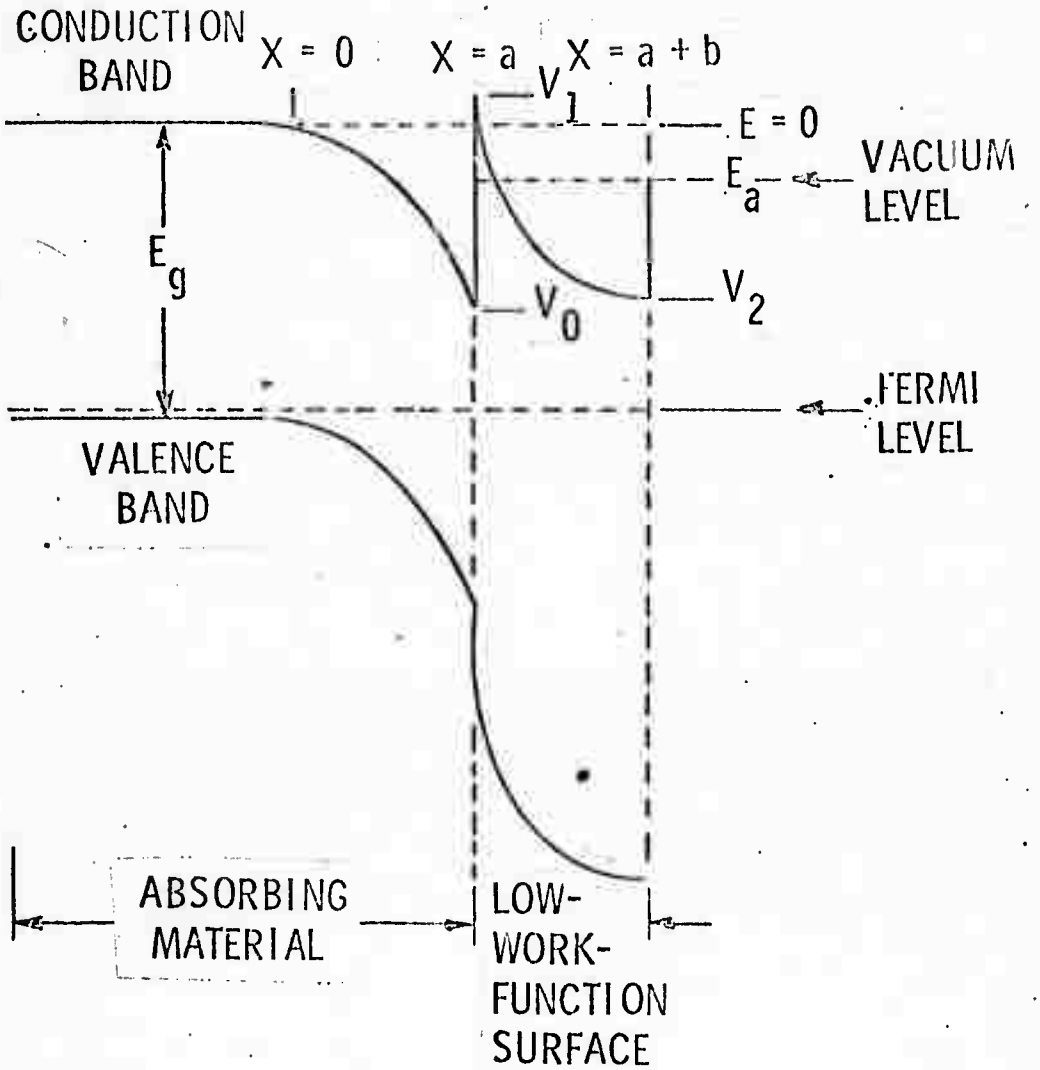

Figure 3 Heterojunction energy-level-diagram used in the calculation of the escape probability.

Photons incident upon the structure from the right will experience reflection at the two barriers. We consider no other attenuation mechanisms for photons with energies less than the surface-material bandgap. The reflection losses are combined, and the fraction of incident photons which penetrates the bulk material is (1 - R).

Monochromatic light with photons of sufficient energy will be absorbed in the bulk region. The process is exponential and characterized by an absorption coefficient α. The absorption coefficients of interest are sufficiently small that the characteristic absorption distance, $1/\alpha$, is much larger than the entire region from the left of the bulk band-bending region to the surface-vacuum interface. The distribution of absorbed photons, and thus generated electrons, if a 1:1 process is assumed, is

$$f(x) = N_o \alpha e^{\alpha(x-a)} \qquad x < a \qquad (1)$$

where N_o is the incident photon density, and a is the position of the surface-bulk interface.

Some of the electrons diffusing and drifting toward the interface will recombine with holes. This loss mechanism is characterized by a recombination length, L, and is exponential in nature. The number of electrons which reach the vacuum interface, if we neglect band structure effects, is

$$\frac{N_o(1-R)}{1 + 1/\alpha L} \qquad (2)$$

The electrons generated by the absorbed photons are "hot"; they have energies greater than the minimum conduction-band energy. Thus, in

addition to recombination, the electrons undergo collisional energy-loss by electron-phonon interaction. This is a random-walk process characterized by the following equation:

$$F = \exp\left[-\left(\frac{\Delta E}{E_i - E_b} \cdot \frac{\ell}{\Delta \ell} \right)^{1/2} \right] \tag{3}$$

where ΔE and $\Delta \ell$ are the mean energy-loss per collision and the mean-free path respectively, E_i and E_b are the initial and barrier energies ($E_i > E_b$), ℓ is the distance to the barrier, and F is the fraction of electrons which overcomes the barrier. From Eq. (3), a distribution of electrons in energy vs. distance is derived.

Since the interface barrier is thin, electrons with insufficient energy to surmount it, may <u>tunnel</u> through the barrier. The WKB approximation for the tunneling probability is

$$P = \exp\left[-\int_{x_o}^{x_1} k\,dx \right], \quad k = \frac{\sqrt{2m(E_b(x) - E)}}{\hbar} \tag{4}$$

where m is the electron mass, $E_b(x)$ is the barrier energy at x, E is the electron energy, $2\pi\hbar$ is Planck's constant, and x_o and x_1 define the tunneling interval. When the expression for the parabolic potential of the surface-layer side of the interface barrier of Figure 3 is substituted into Eq. 4, the tunneling probability becomes:

$$P = \exp\left[-\frac{\sqrt{2m(V_1 - V_2)}\,(b-a)}{\hbar} \left\{ \left(1 - \frac{E-V_2}{V_1-V_2} \right)^2 - \left(\frac{E-V_2}{V_1-V_2} \right) \ln\left(1 + \left(\frac{V_1-V_2}{E-V_2} - 1 \right)^2 \right) \right\} \right] \tag{5}$$

All electrons reaching the surface barrier with energies less than that of the surface barrier are lost. For those with energy greater than that of the surface barrier we calculate the quantum mechanical reflection coefficient. The non-reflected portion of the sufficiently-energetic electrons which arrive at the surface-layer-vacuum interface escape into vacuum.

The hot-electron energy-loss, and the curved-band bulk-region ($o < x < a$) cause the electrons to be distributed in energy. To perform the calculation, distributions must be calculated at $x = o$, $x = a$, at the parabolic edge of the interface barrier, and at $x = a + b$. Each distribution is dependent upon the preceding one. To simplify the calculation, the initial electron-distribution may be approximated by the following expressions:

$$F(x) = \begin{cases} N_o \alpha & -(1/\alpha - a) < x < a \\ 0 & \text{otherwise} \end{cases} \qquad (6)$$

In addition, numerical integrals are required at several points. Because of the involved nature of the calculation, a computer program was written to perform the evaluation. With this program, it is a straightforward matter to evaluate photoemission efficiency as a function of any parameter in the model.

The parameter values used are in accord with accepted values. The width of the curved-band bulk-region is 100Å; that of the surface layer was assumed to be 30Å. Referring to Figure 3, V_o was taken to be -0.3 eV.[5,2]

V_1 was chosen so that the internal-barrier height as measured from the Fermi level is 1.17 eV.[2] V_2 and E_a were also chosen to be in accord with the experimental results.[5] The mean-free paths were taken to be 50Å and 10Å in the bulk and surface regions respectively. The electron energy-loss per collision is .05 eV. The absorption and reflection coefficients were calculated from known values for the binary materials. The recombination length depends on the quality of the actual material, and was chosen accordingly. The reflection coefficient and the recombination length are needed only to calculate the quantum efficiency, which is the escape probability multiplied by the factor of Equation 2. For escape-probability calculations, these two parameters are not required.

As previously noted, the problem is constrained to be one dimensional. No account has been taken of thermal excitation of electrons over the interface barrier, nor was Schottky-barrier lowering considered. Hot-electron energy-loss is neglected in the tunneling region. While the surface region is at most ten atomic layers thick, it is treated as a bulk semiconductor. The band-bending regions are assumed to be parabolic.

A comparison of the theoretical and experimental wavelength-dependence of the electron escape-probability for negative-electron-affinity photoemitters is shown in Figure 4. Curve (1) is generated from a collection of experimental estimates of the escape probability, and curves (2) and (3) represent respectively the theoretical escape-probability when it is assumed that the interface barrier height is 1.17 eV, independent of wavelength (Curve 2), or (Curve 3) varies in the manner shown in reference 2. The experimental point at 0.9 microns is for GaAs and reflects the spread in escape probability obtained by different investigators.[3,13] The next five escape probabilities are for $Ga_{1-x}In_xAs$ and are taken from Fisher et al.[3] The point at 1.4 microns is an estimate of the experimental escape probability for our $InAs_{0.4}P_{0.6}$, discussed in Section 1.0.

(Curve 1) wavelength dependence of the electron escape probability of NEA photoemitters.

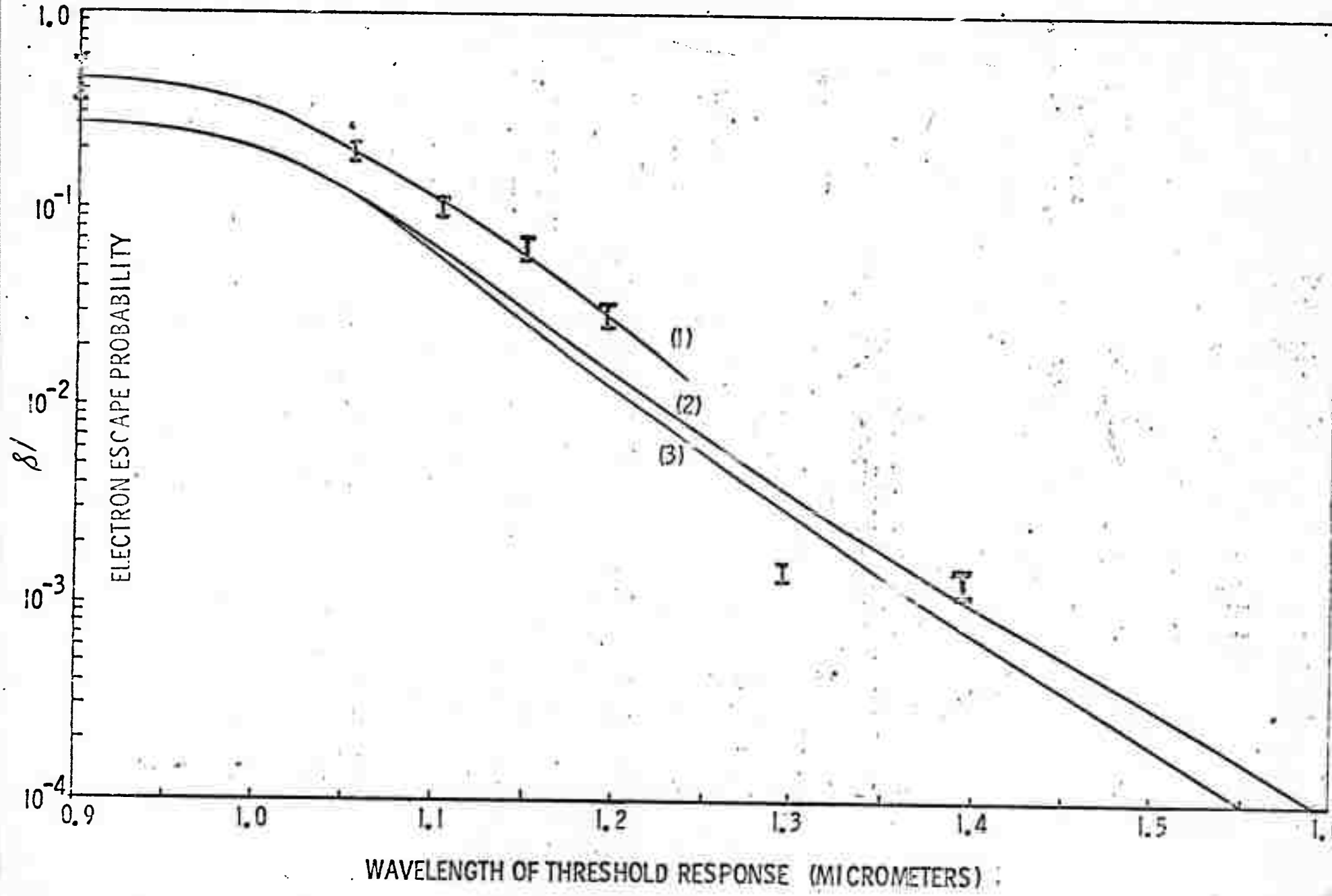

Quantitatively, the experimental and theoretical curves are within a factor of two over the range from 0.9 microns to 1.2 microns. The qualitative agreement is equally encouraging. Consequently, the fact that "bandgap-limited" photoemission has been observed out to 1.3 microns[3,12] or even 1.4 microns (Section 1.0) can not be taken as evidence against the heterojunction interpretation for NEA cathodes. If anything, (as shown in Figure 4) this could be taken as evidence in favor of the heterojunction model.

Clearly, the issue involving the interpretation of the Cs-O low-work-function surface is not settled. To our knowledge the only evidence which appears to contradict the heterojunction model is the evidence that the thickness of the low work-function layer may be of monolayer dimensions. It is difficult to see how the low-work-function properties of Cs-O could be explained in terms of the bulk properties of Cs_2O (as in the heterojunction model) when only one or two monolayers of the material are present. However, for the thickness determination, it is assumed that the bulk density of Cs and Cs_2O characterize the low-work-function surface. Although this may be a reasonable assumption, it has not been verified[14]. Direct measurements of the thickness of optimized Cs-O low-work-function surfaces could settle this point.

Because of the good agreement between experiment and theory, we can predict that for $Ga_{1-x}In_xAs$ and $InAs_{1-x}P_x$ NEA cathodes utilizing Cs-O low-work-function surfaces, the peak quantum efficiency at 1.5 microns will be at best on the order of 0.01%.

3.0 MATERIALS GROWTH

In the last quarter we have successfully grown GaAs on Ge, Spinel and GaAs substrates. Gallium diethyl chloride was used as the Ga source. For the Arsine source, a 5% min of Arsine in high-purity H_2 was used. Gas-phase etching occurs in the reaction mixture if the substrate temperature is above 750°C. Growth takes place near 600°C.

The best results so far were obtained in a vertical rf-heated, flow-type reactor, constructed of quartz, Teflon and stainless steel. The temperature of the pyrolytic graphite susceptor is monitored optically with a Ratek Infrared Thermometer, as well as with a thermocouple embedded in the graphite susceptor in close proximity to the substrate. Before deposition, the substrates are heated to 750°C for 10 minutes to remove surface contamination. The temperature is then lowered to 600°C and GaAs grown for about 90 minutes.

GaAs material grown by this method was comparable to bulk material. However, we have experienced difficulty with reproducibility. Figure 5 shows a photoluminescence spectrum of one of our GaAs layers grown on a Ge substrate.

In the coming period we should be able to eliminate the problems with reproducibility and get the doping and thickness parameters under control.

Figure 5 Photoluminescence spectrum of epitaxial GaAs on Ge

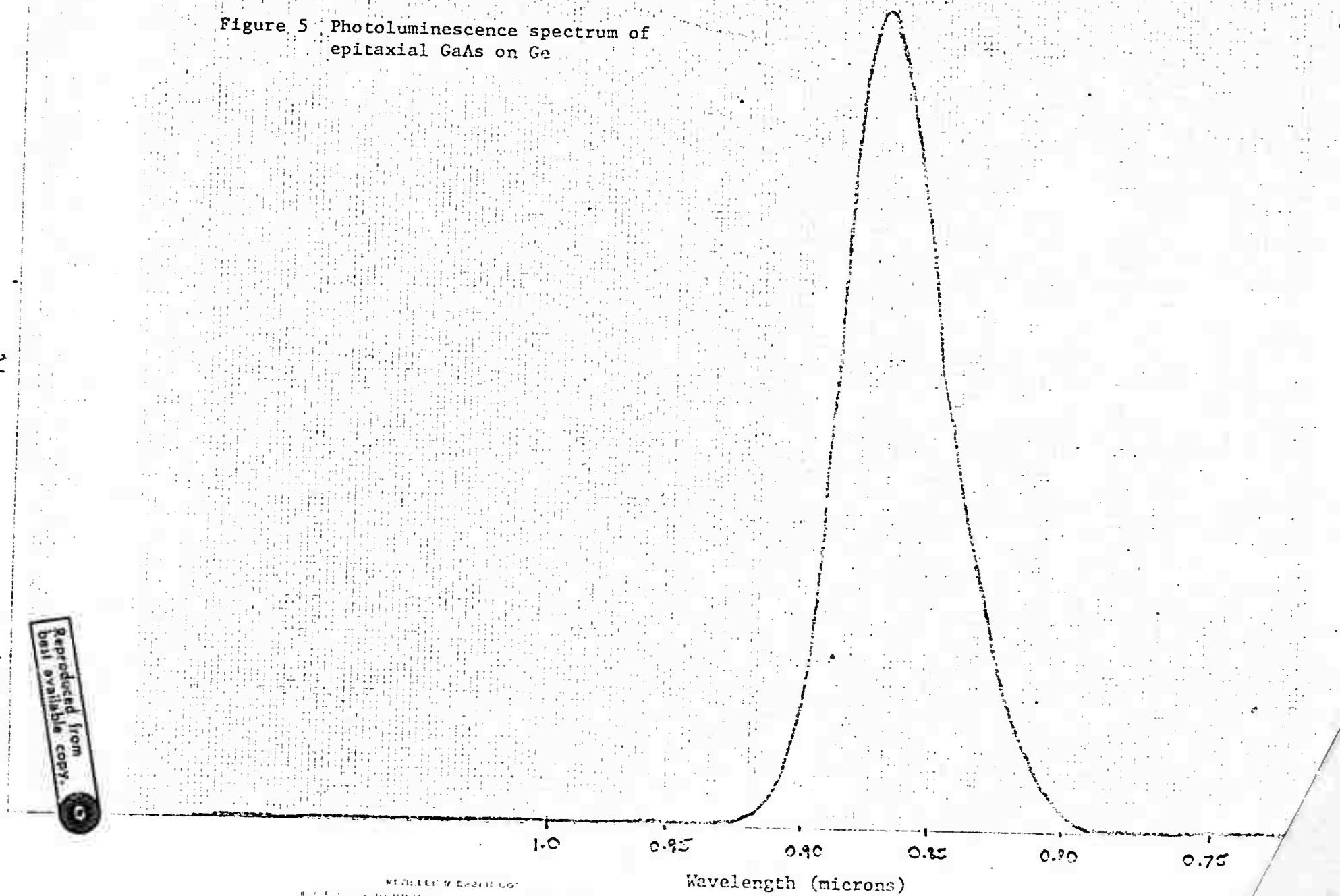

REFERENCES

1. H. Sonnenberg, Appl. Phys. Lett. 16, 245 (1970)
2. L. W. James, G. A. Antypas, J. J. Uebbing, T. O. Yep, and R. L. Bell, Journ. Appl. Phys. 42, 580 (1971).
3. D. G. Fisher, R. E. Enstrom, and F. F. Williams, Appl. Phys. Lett. 18, 371 (1971).
4. H. Sonnenberg, Appl. Phys. Lett. 14, 289 (1969).
5. J. J. Uebbing and L. W. James, Journ. Appl. Phys. 41, 4505, (1970).
6. A. H. Sommer, H. H. Whitaker, and B. F. Williams, Appl. Phys. Lett. 17, 273 (1970).
7. The ratio purposely contains a constant multiplier Y to reflect the fact that we do not know the absolute calibration of our partial pressure analyzer, and furthermore to account for the large discrepancy in the literature as to the Cs coverage required for optimum yield. For example, S. Garbe, Solid State Electron. 12, 893 (1969) measures 3×10^{14} Cs/cm^2 for GaAs and T. E. Fischer, Phys. Rev. 142, 519 (1966) measures 1×10^{15} Cs/cm^2 for InP.
8. A monolayer of Cs is arbitrarily defined as the coverage required to optimize the photoresponse with Cs only.
9. Experiments with much thicker Cs-O films confirm that the ratio remains constant when it is assumed that slightly less than a monolayer of Cs remains unconverted.
10. L. W. James and J. J. Uebbing, Appl. Phys. Lett. 16, 370 (1970).
11. J. D. Taynai and H. Sonnenberg, to be published.
12. Brown F. Williams and J. J. Tietjen, Proc. IEEE 59, 1489 (1971).
13. S. Garbe, Solid-State Electronics 12 893 (1969).
14. A "fluffy" form of Cs_2O with a much lower density could possibly remove the apparent thickness-objection to the heterojunction model.